Molecular Simulation Study on the Interaction between Tyrosinase and Flavonoids from *Sea Buckthorn*

Xiaofang Li, Jun Guo, Jiaqi Lian, Feng Gao, Abdul Jamil Khan, Tegexibaiyin Wang,* and Feng Zhang*

Read Online

ACCESS | Metrics & More | Article Recommendations

ABSTRACT: Isorhamnetin, kaempferol, myricetin, and quercetin are four kinds of secondary metabolites in sea buckthorn, which have a wide range of biological activities. Investigating their interactions with tyrosinase at the atomic level can improve the bioavailability of sea buckthorn. Both molecular docking and molecular dynamics simulation methods were employed to study the interactions of these ligands with tyrosinase. The results of molecular docking indicated that these four small molecules such as isorhamnetin, kaempferol, myricetin, and quercetin can all dock into the active center of tyrosinase, and by occupying the active site, they can prevent substrate binding, thereby reducing the catalytic activity of tyrosinase. Molecular dynamics simulation trajectory analysis showed that all tyrosinase−ligand complexes reach an equilibrium within 100 ns. In addition, quercetin has the lowest binding energy among these four ligands, and the complex with tyrosinase is the most stable. This study not only provides valuable information for improving the bioavailability of sea buckthorn but also contributes to the discovery of effective natural inhibitors of tyrosinase.
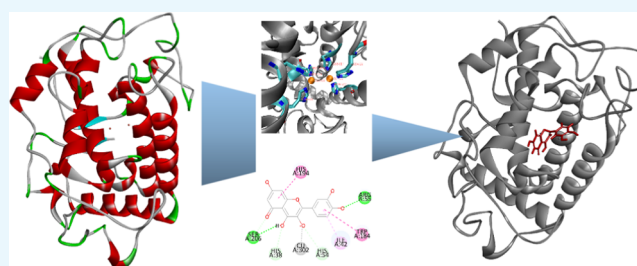
1. INTRODUCTION

Natural products normally show low toxicity and high efficiency to be used as chemopreventive agents. Sea buckthorn (*Hippophae rhamnoides* L.) belongs to the genus Hippophae and Elegancies family and is mainly distributed in Russia, Mongolia, and China.[1] It exhibits many bioactivities, such as antitumour, antioxidation, anti-inflammatory, antiradiation, and so on. It is a traditional Chinese medicine used in ancient Tibetan and Mongolian medicine. Previous studies have shown that the fruits, leaves, and stem bark of sea buckthorn contain more than 190 natural active substances such as vitamins, flavonoids, lycopene, and carotenoids, which are all beneficial for human health.[2] Flavonoid is one of the most important secondary metabolites in sea buckthorn, which has a range of anti-inflammatory and antimicrobial effects.[3] In addition, some flavonoids also show antiviral and anticancer properties.[1] Isorhamnetin, kaempferol, myricetin, and quercetin are the four major flavonoids in sea buckthorn (Figure 1).

Isorhamnetin is a flavonoid that widely exists in sea buckthorn, Ginkgo biloba, mulberry cotyledon, and other plants. It is commonly used in the prevention and treatment of cardiovascular diseases[4] and has many functions such as anti-hepatotoxicity, antioxidation, and inhibition of platelet aggregation. Recent studies have shown that isorhamnetin can prevent the H_2O_2-induced oxidative damage in H9c2 cardiomyocytes.[5]

Kaempferol has been found in many edible plants (such as tea, cauliflower, strawberry, and grape), which is commonly used in traditional Chinese medicine. Some epidemiological studies have found that long-term consumption of kaempferol can possibly reduce the risk of cancer and cardiovascular disease.[6]

Myricetin is a common metabolite in natural foods such as berries, vegetables, tea, wine, and herbs. It has been considered as an antioxidant that can inhibit the free radical-mediated photoaging of the skin.[7] Some studies reveal that myricetin can inhibit weight gain and body fat accumulation by increasing fatty acid oxidation.[8]

Quercetin exhibits protective effects on the cardiovascular system. Quercetin and other flavonoids can protect low-density lipids (LDL) from oxidation, inhibit atherosclerotic plaque formation,[9] and resist hypertension and arrhythmia by promoting the relaxation of cardiovascular smooth muscle.[10]

Tyrosinase, a multifunctional copper-containing metal enzyme, is commonly located on the membrane of melanosomes and widely exists in animals, plants, and microorganisms.[11] Structurally, tyrosinase is composed of multiple subunits, each subunit contains two copper ions
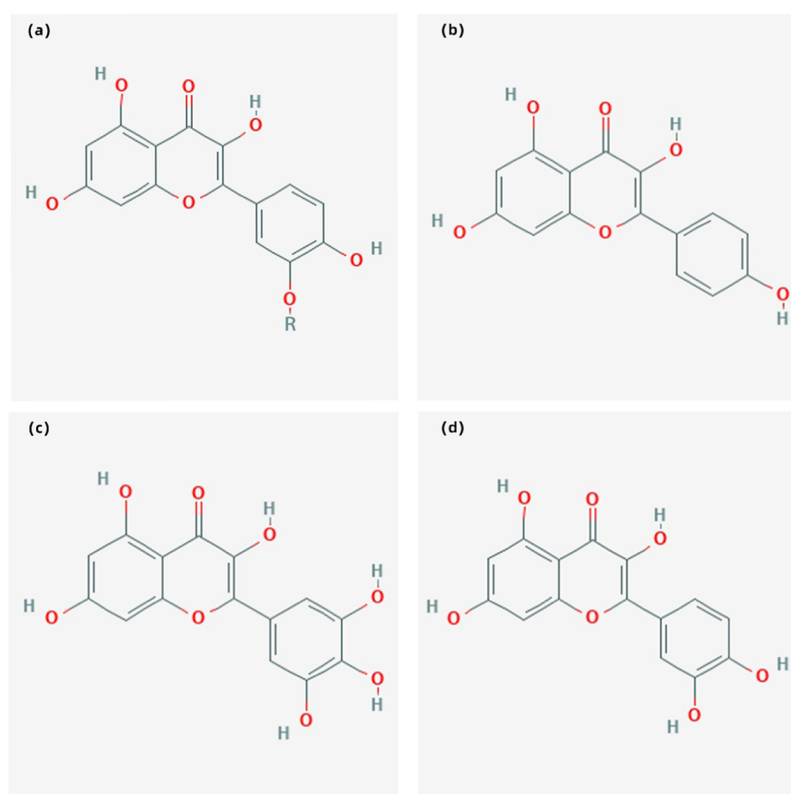
Figure 1. Chemical structures of (a) isorhamnetin, (b) kaempferol, (c) myricetin, and (d) quercetin.
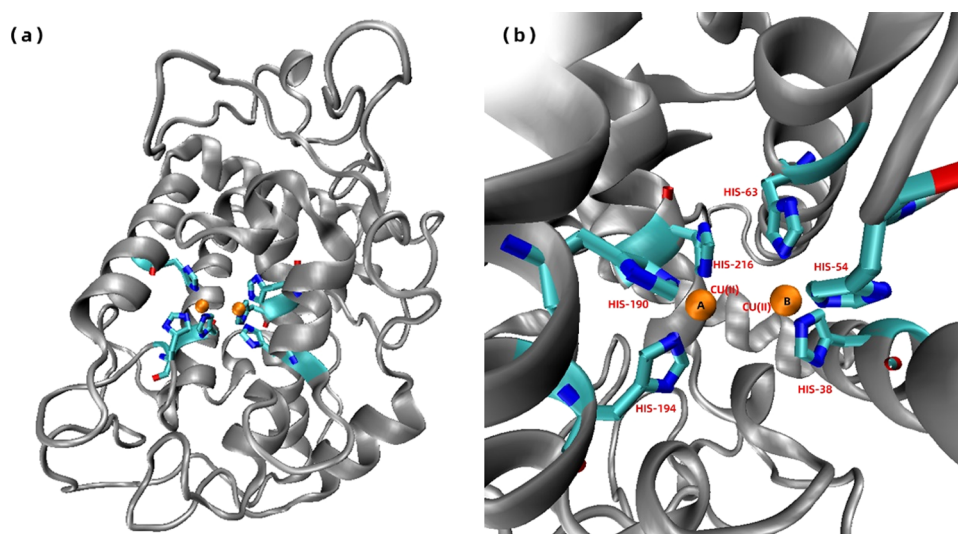
Figure 2. (a) High-resolution (1.33 Å) crystal structure of mushroom tyrosinase (PDB ID: 2zmxc A chain). (b) Active site of the enzyme contains two copper ions denoted as A and B, which are coordinated by six histidine residues HIS38, HIS54, HIS63 (CuII (a)) and HIS190, HIS194, HIS216 (CuII (b)), respectively, and depicted by a rod model.

surrounded by three histidine residues, which are responsible for the catalytic activity of tyrosinase (Figure 2). In addition, an endogenous bridge connects the two copper ions to form the active center of tyrosinase.[12] The enzymatic reaction of tyrosinase is the primary process in melanin production in living organisms, where the accumulation of an excessive level of melanin can cause skin damage, such as age spots or malignant melanoma. Moreover, the browning of fruits and vegetables is related to the oxidation of phenolic compounds catalyzed by tyrosinase, which results in a loss of market value

of foods.[13] Therefore, tyrosinase inhibitors have gradually become a research hotspot.

Molecular docking has been an important approach to investigate protein−ligand interactions.[14] Molecular dynamics simulation is usually used to obtain the interaction trajectories for better understanding biological processes, which has been considered as a general method to study the interactions and conformational stability of biomolecules.[15] In this study, we studied the protein conformation changing of tyrosinase upon interacting with four kinds of flavonoids such as isorhamnetin,
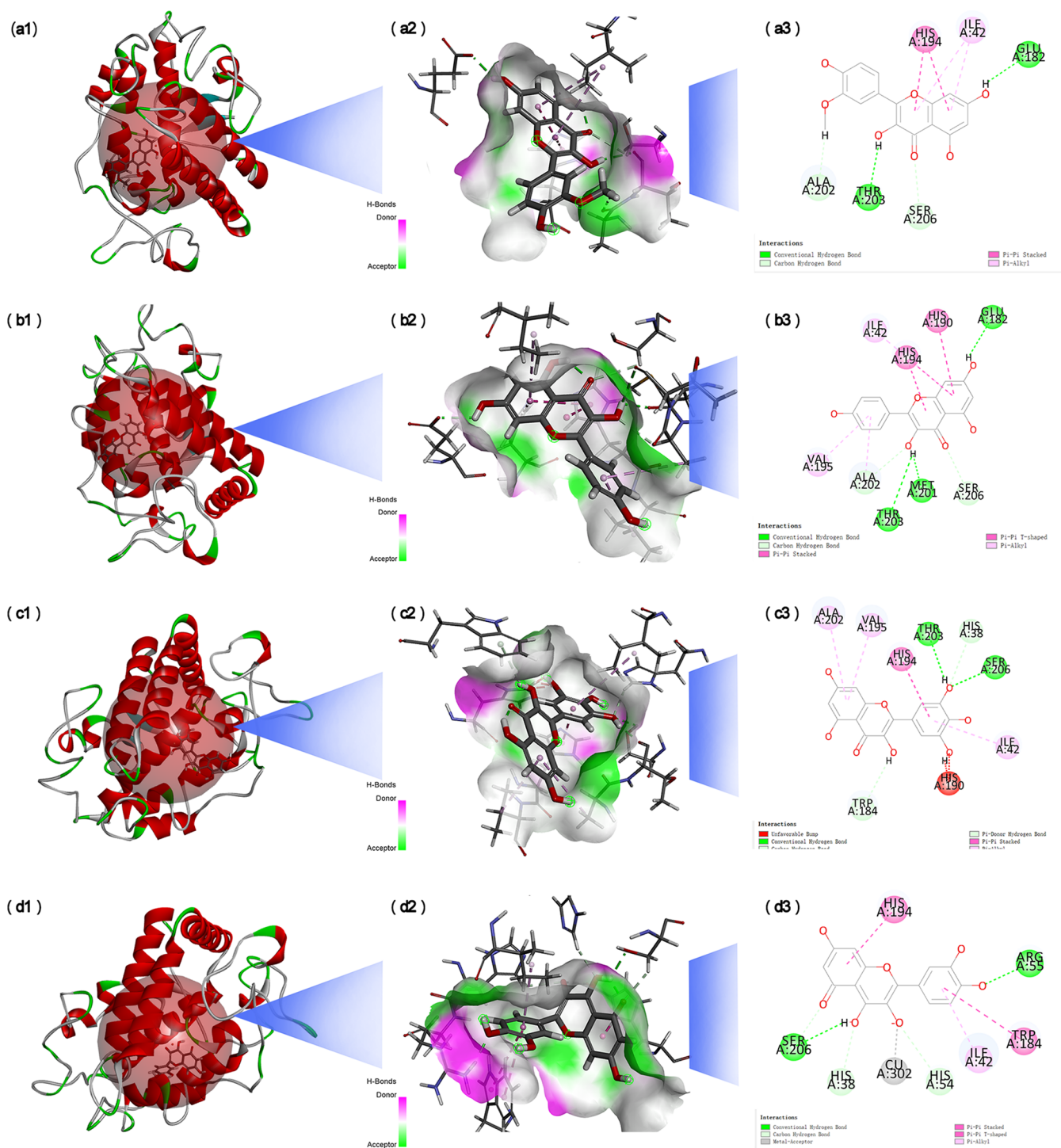
Figure 3. Docking position and interactions of tyrosinase with four ligands: (a) isorhamnetin, (b) kaempferol, (c) myricetin, and (d) quercetin. The numbers 1−3 represent the binding site, binding conformation, and interactions diagram between ligands and tyrosinase, respectively.

kaempferol, myricetin, and quercetin by molecular docking and molecular dynamics simulation. The authors propose that searching new bioactive ligands to reduce the biocatalytic activity of tyrosinase will be of great significance in biotechnology and pharmacology, which will not only help better understand the bioactivities of tyrosinase itself,[16] but also pave the way for the drug discovery of tyrosinase inhibitors.

2. MATERIALS AND METHODS

2.1. Preparation of Tyrosinase and the Four Small Molecules. The crystal structure of tyrosinase (PDB ID: 2zmx A chain) was obtained from Brookhaven Protein Database (http://www.rcsb.org/pdb). The R value of this file is 0.213, and the protein crystal was prepared at pH 7.5. Discovery Studio (DS, Dassault Systems BIOVIA, USA), which is the professional molecular simulation software, was used to pretreat protein receptors, including deleting unnecessary ligands and water molecules, hydrogenation, and completing
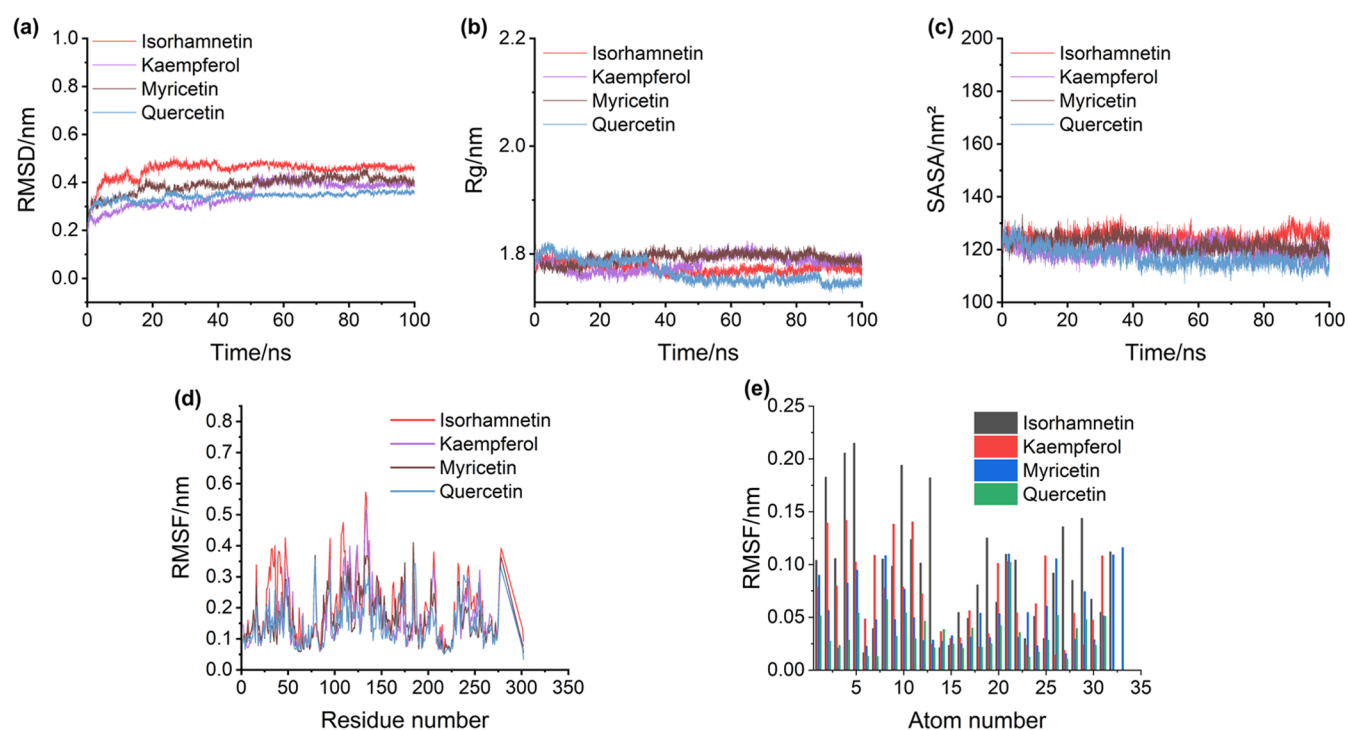
Figure 4. Molecular dynamics (100 ns) results of four tyrosinase−ligand complexes. (a) RMSD, (b) Rg, (c) SASA, and (d) RMSF values of four kinds of tyrosinase without ligand were plotted according to the residue number, and (e) RMSF values of four tyrosinase ligands were plotted according to the number of atoms.

incomplete amino acid residues.[17] Three-dimensional (3D) transformer of the four small molecules downloaded from PubChem database (http://publichem.ncbi.nlm.nih.gov), and the registration numbers for flavonoid ligands isorhamnetin, kaempferol, myricetin, and quercetin are 5281654, 5280863, 5281672, and 5280343, respectively. The topology was built using the PRODRG2 server.[18] DS software was used to optimize the geometry of small-molecule ligands. Both protein receptors and small-molecule ligands are endowed to the CHARMM force field.

2.2. Molecular Docking. Tyrosinase is composed of 277 amino acids and two Cu ions. A sphere with a radius of 12 Å was set up. DS software was used to view and analyze the flexible docking results. During the whole docking process, amino acid residues such as HIS38, HIS54, HIS63, HIS180, HIS190, HIS194, HIS215, and HIS216 in the protein receptor are all set flexible,[19] and the rest remains a rigid structure. The binding energy was considered the optimal docking posture of small-molecule ligands, and the minimum binding energy of protein complexes was selected for further analysis.

2.3. Molecular Dynamics (MD) Simulation. The lowest binding free energy conformation of each complex was considered to be the initial conformation for the MD study.[20] The results of the MD simulation can explain the conformational changes of the protein complex during the binding process. Moreover, they further provided the basis for the binding mode of small-molecule ligands and receptor proteins.[21] All MD simulations in the current work used the GROMACS (version 19.5) with the GROMACS96 43a1 force field.[22] Dundee PRODRG2.5 server was used to generate the topological parameters of small molecules. The minimum distance between any solute atoms and the edge of the periodic box is 1.0 nm.[23] The box was filled with extended single-point charge (SPC), water molecules, and solvation system; then,

counter ions were added to neutralize the total charge of the system. After minimizing the energy, the system was balanced in two steps: (1) canonical ensemble (NVT, 0.2 ns) and (2) isothermal isobaric (NPT, 0.2 ns). Finally, 100 ns MD simulation was performed at 1 bar and 300 K,[24] and the atomic coordinates were recorded in the trajectory file at every 0.1 ps for subsequent analysis. Finally, full binding was used to prevent the ligand from drifting in molecular dynamics, and the Cu ions in tyrosinase were constrained. After MD simulation, the trajectory was analyzed using GROMACS (version 19.5).

3. RESULTS AND DISCUSSION

3.1. Molecular Docking. The interactions mechanism between tyrosinase and four small-molecule ligands was studied by DS software. Figure 3a1−d1 shows the optimal docking conformation between tyrosinase and ligands. During the docking process, the four ligands were inserted into the active site of tyrosinase to form a relatively stable binding conformation 3a2−d2, and the binding energy of quercetin with tyrosinase is −586.7 kcal/mol, myricetin is −165.3 kcal/mol, kaempferol is −111.7 kcal/mol, and isorhamnetin is −75.7 kcal/mol. Generally speaking, the protein lumen can provide a strong hydrophobic environment and multiple hydrogen-bonding sites for ligands, which contributes to the stability of ligands. Therefore, the interactions between tyrosinase and four small-molecule ligands were analyzed by DS, and the results are shown in Figure 3a3−d3.

Isorhamnetin, kaempferol, myricetin, and quercetin all can interact with tyrosinase active sites by conventional hydrogen bonds, carbon−hydrogen bonds, Pi−Pi stacking, and Pi−alkyl interactions. Except for the above, HIS190 and myricetin show the effect of unfavorable bump, while Cu302 and quercetin exhibit the effect of a metal acceptor. The binding energy between quercetin and tyrosinase is 4−8 times higher than that

of the other three small molecules, or it may be due to the interactions between quercetin and Cu ions in the active center of tyrosinase. Therefore, the inhibitory effect of quercetin on tyrosinase is better than those of others.

3.2. MD Simulation Trajectory Analysis. Although the interactions between tyrosinase and four small-molecule ligands have been studied by the molecular docking method, except quercetin, the difference between them is not significant. Therefore, a 100 ns MD simulation method was used to further compare the differences of the four complexes at the molecular level. The stability and degree of the interactions between tyrosinase and four small molecules were further elucidated using GROMACS program. The dynamic properties of the four complexes were then subjected to analysis of the trajectory data obtained from the 100 ns MD simulations. Root mean square deviation (RMSD), radius of gyration (Rg), solvent accessible surface area (SASA), and root mean square fluctuation (RMSF) were used to evaluate each system in the molecular dynamics studies, and the results are shown in Figure 4.

3.2.1. Root Mean Square Deviation. RMSD is used to determine the average deviation between the conformation of the complex and the original conformation at a specific time and to evaluate whether the complex system has reached a stable state.[25] As shown in Figure 4, during the simulation, the RMSD value of the isorhamnetin−tyrosinase complex configuration kept increasing until it stabilized at approximately 0.45 nm after 40 ns. Similarly, the RMSD value of the kaempferol−tyrosinase and myricetin−tyrosinase complexes finally reached an RMSD plateau at approximately 0.4 nm after 50 ns. Meanwhile, the RMSD value of the quercetin/tyrosinase complex rapidly reached approximately 0.38 nm after 25 ns, although the complex underwent small fluctuations during the periods between 15 and 25 ns, it is the least volatile of the four complexes. These results indicated that the four systems reached a steady state at the end of the MD simulations. Fortunately, the complex of quercetin and tyrosinase was stable within 25 ns, and its equilibrium speed was faster. The RMSD value was 0.3 nm. In conclusion, the four complexes are stable, and quercetin is the most.

3.2.2. Radius of Gyration. The time evolution of the radius of gyration (Rg) is an excellent assessment of the protein collapse dynamics.[26] The radius of gyration of the four systems was quantified and the relationship between the radius of gyration and the simulation time was plotted to check the protein compactness,[27] as shown in Figure 4b. The Rg of all of the systems reached a constant value at approximately 40 ns, indicating that MD simulation reached an equilibrium after 40 ns. The Rg values of isorhamnetin−tyrosinase, kaempferol−tyrosinase, and myricetin−tyrosinase complexes did not change significantly throughout the simulation and kept fluctuating at 1.75, 1.77, and 1.8 nm, respectively, indicating that the binding region shows little influence on their structures. The Rg value of the quercetin−tyrosinase complex shows a downward trend during the whole 100 ns of simulation, while the average Rg value is 1.77 ± 0.02 nm, indicating that their structure became more compact after MD simulation. The results show that the gyration radius of the quercetin−tyrosinase complex is smaller than those of the other three systems, indicating that the structural tightness of the quercetin−tyrosinase complex was better than those of other systems.

3.2.3. Solvent Accessible Surface Area. Theoretically, SASA can be used as a parameter to describe the protein solvent interactions ratio that predicts the degree of conformational changes in the binding processes and can be used to evaluate the protein accessibility.[28] During the 100 ns simulation time, the SASA of the system changes as shown in Figure 4c. The SASA of isorhamnetin−tyrosinase, kaempferol−tyrosinase, and myricetin−tyrosinase fluctuated within the range of 125−130, 115−125, and 120−130 nm, respectively, while the SASA of quercetin−tyrosinase showed a slightly oscillatory downward trend during MD simulation. The SASA of quercetin−tyrosinase decreased rapidly from 130 to 110 nm, respectively, and maintained an equilibrium after 40 ns. This indicates that the combination of quercetin makes the structure of tyrosinase more compact. The result of SASA is consistent with that of Rg, which confirms the correctness of MD simulation.

3.2.4. Root Mean Square Fluctuation. To assess the mobility of local proteins, the time-averaged root mean square fluctuation (RMSF) values of tyrosinase residues in the absence and presence of ligands were calculated and plotted against residue numbers at the simulation trajectory, as shown in Figure 4d. The RMSF values of the neat tyrosinase were generally higher than those of the four ligands, indicating that the binding of ligands restricted the fluctuations of tyrosinase. The results show that the fluctuation greater than 0.4 nm corresponds to the residues far away from the ligand-binding site. In addition, the residue contacting with the ligand is the most stable one, and the RMSF value is low.

In addition, the RMSF of the four ligand atom positions were calculated to check their conformational changes, as shown in Figure 4e. The results show that the fluctuation of four ligand atoms was limited (<0.22 nm). Therefore, it can be concluded that the interactions between tyrosinase and the four ligands were stable during the simulation.

4. CONCLUSIONS

In this paper, the interactions of four small-molecule ligands with tyrosinase were studied by both molecular docking and molecular dynamics simulation. According to the results of molecular docking, isorhamnetin, kaempferol, myricetin, and quercetin were bound in the cavity of tyrosinase. The affinity of tyrosinase to sea buckthorn ligands can be in the order quercetin > myricetin > kaempferol > isorhamnetin. Hydrophobicity, hydrogen bond, and Pi−Pi stacking interactions played major roles in the stability of tyrosinase−ligand complexes. Quercetin was found to be the strongest ligand to tyrosinase, which could be ascribed to the additional nonbonding force between quercetin and Cu ions of tyrosinase. Molecular dynamics simulation shows that tyrosinase−ligand complexes were stable within 50 ns. Since small molecules interact with two copper ions of tyrosinase, better inhibitors could be artificially designed in the future. It can be clearly seen that both Rg and SASA values of the quercetin−tyrosinase complex are smaller than those of the other three systems, which indicates that the binding energy of the quercetin−tyrosinase complex is the lowest in the molecular docking results. In addition, the atom fluctuation curve shows that the interactions between tyrosinase and four ligands are stable within the simulation time. The results of molecular dynamics simulation are consistent with those of molecular docking, which further proves the accuracy of docking results.

■ AUTHOR INFORMATION

Corresponding Authors

Tegexibaiyin Wang − *Pharmacy Laboratory, Inner Mongolia International Mongolian Hospital, Hohhot 010065, China;* Email: tegexibaiyin@yeah.net

Feng Zhang − *Biomedical Nanocenter, School of Life Science, Inner Mongolia Agricultural University, Hohhot 010011, China; Terahertz Technology Innovation Research Institute, Shanghai Key Laboratory of Modern Optical System, Terahertz Science Cooperative Innovation Center, University of Shanghai for Science and Technology, Shanghai 200093, China; Wenzhou Institute, University of Chinese Academy of Sciences, Wenzhou 325001, China; Pharmacy Laboratory, Inner Mongolia International Mongolian Hospital, Hohhot 010065, China; State Key Laboratory of Respiratory Disease, Guangzhou Institute of Oral Disease, Stomatology Hospital, Department of Biomedical Engineering, School of Basic Medical Sciences, Guangzhou Medical University, Guangzhou 511436, China;* ⊙ orcid.org/0000-0001-6035-4829; Email: fengzhang1978@hotmail.com

Authors

Xiaofang Li − *Biomedical Nanocenter, School of Life Science, Inner Mongolia Agricultural University, Hohhot 010011, China*

Jun Guo − *Terahertz Technology Innovation Research Institute, Shanghai Key Laboratory of Modern Optical System, Terahertz Science Cooperative Innovation Center, University of Shanghai for Science and Technology, Shanghai 200093, China;* ⊙ orcid.org/0000-0001-6944-0731

Jiaqi Lian − *Wenzhou Institute, University of Chinese Academy of Sciences, Wenzhou 325001, China*

Feng Gao − *Biomedical Nanocenter, School of Life Science, Inner Mongolia Agricultural University, Hohhot 010011, China*

Abdul Jamil Khan − *Biomedical Nanocenter, School of Life Science, Inner Mongolia Agricultural University, Hohhot 010011, China*

Complete contact information is available at:
https://pubs.acs.org/10.1021/acsomega.1c02593

Notes

The authors declare no competing financial interest.

■ REFERENCES

(1) Nijveldt, R. J.; van Nood, E.; van Hoorn, D. E.; Boelens, P. G.; van Norren, K.; van Leeuwen, P. A. Flavonoids: a review of probable mechanisms of action and potential applications. *Am. J. Clin. Nutr.* **2001**, *74*, 418−425.

(2) Patel, C. A.; Divakar, K.; Santani, D.; Solanki, H. K.; Thakkar, J. H. Remedial Prospective of *Hippophae rhamnoides* Linn. (Sea Buckthorn). *ISRN Pharmacol.* **2012**, *2012*, No. 436857.

(3) Tim Cushnie, T. P.; Lamb, A. J. Antimicrobial activity of flavonoids. *Int. J. Antimicrob. Agents* **2005**, *26*, 343−356.

(4) Sun, J.; Sun, G.; Meng, X.; Wang, H.; Luo, Y.; Qin, M.; Ma, B.; Wang, M.; Cai, D.; Guo, P.; Sun, X. Isorhamnetin protects against doxorubicin-induced cardiotoxicity in vivo and in vitro. *PLoS One* **2013**, *8*, No. e64526.

(5) Sun, B.; Sun, G. B.; Xiao, J.; Chen, R. C.; Wang, X.; Wu, Y.; Cao, L.; Yang, Z. H.; Sun, X. B. Isorhamnetin inhibits HO-induced activation of the intrinsic apoptotic pathway in H9c2 cardiomyocytes through scavenging reactive oxygen species and ERK inactivation. *J. Cell. Biochem.* **2012**, *113*, 473−485.

(6) Calderon-Montano, J. M.; Burgos-Moron, E.; Perez-Guerrero, C.; Lopez-Lazaro, M. A review on the dietary flavonoid kaempferol. *Mini-Rev. Med. Chem.* **2011**, *11*, 298−344.

(7) Huang, J. H.; Huang, C. C.; Fang, J. Y.; Yang, C.; Chan, C. M.; Wu, N. L.; Kang, S. W.; Hung, C. F. Protective effects of myricetin against ultraviolet-B-induced damage in human keratinocytes. *Toxicol. In Vitro* **2010**, *24*, 21−28.

(8) Chang, C. J.; Tzeng, T. F.; Liou, S. S.; Chang, Y. S.; Liu, I. M. Myricetin Increases Hepatic Peroxisome Proliferator-Activated Receptor α Protein Expression and Decreases Plasma Lipids and Adiposity in Rats. *Evidence-Based Complementary Altern. Med.* **2012**, *2012*, No. 787152.

(9) Formica, J. V.; Regelson, W. Review of the biology of Quercetin and related bioflavonoids. *Food Chem. Toxicol.* **1995**, *33*, 1061−1080.

(10) Rivera, L.; Moron, R.; Sanchez, M.; Zarzuelo, A.; Galisteo, M. Quercetin ameliorates metabolic syndrome and improves the inflammatory status in obese Zucker rats. *Obesity* **2008**, *16*, 2081−2087.

(11) Xie, L. P.; Chen, Q. X.; Huang, H.; Wang, H. Z.; Zhang, R. Q. Inhibitory Effects of Some Flavonoids on the Activity of Mushroom Tyrosinase. *Biochemistry* **2003**, *68*, 487−491.

(12) Ismaya, W. T.; Rozeboom, H. J.; Weijn, A.; Mes, J. J.; Dijkstra, B. W.; et al. Crystal Structure of Agaricus bisporus Mushroom Tyrosinase: Identity of the Tetramer Subunits and Interaction with Tropolone. *Biochemistry* **2011**, *50*, 5477−5486.

(13) Quispe, Y. N. G.; Hwang, S. H.; Wang, Z.; Lim, S. S. Screening of Peruvian Medicinal Plants for Tyrosinase Inhibitory Properties: Identification of Tyrosinase Inhibitors in Hypericum laricifolium Juss. *Molecules* **2017**, *22*, No. 402.

(14) Morris, G. M.; Lim-Wilby, M. Molecular docking. *Methods Mol. Biol.* **2008**, *443*, 365−382.

(15) Rapaport, D. C.; Blumberg, R. L.; Mckay, S. R.; Christian, W. The Art of Molecular Dynamics Simulation. *Comput. Phys.* **1999**, *10*, No. 456.

(16) Choi, Y. K.; Duran, T.; Im, W. CHARMM-GUI Synthetic Polymer Modeler for Modeling and Simulation of Synthetic Polymers. *Biophys. J.* **2019**, *116*, 572a.

(17) Gao, Y. D.; Huang, J. F. An extension strategy of Discovery Studio 2.0 for non-bonded interaction energy automatic calculation at the residue level. *Zool. Res.* **2011**, *32*, 262−266.

(18) Schüttelkopf, A.; Aalten, D. PRODRG: a tool for high-throughput crystallography of protein−ligand complexes. *Acta Crystallogr.* **2004**, *60*, 1355−1363.

(19) Matoba, Y.; Kumagai, T.; Yamamoto, A.; Yoshitsu, H.; Sugiyama, M. Crystallographic Evidence That the Dinuclear Copper Center of Tyrosinase Is Flexible during Catalysis. *J. Biol. Chem.* **2006**, *281*, 8981−8990.

(20) Pan, F.; Li, J.; Zhao, L.; Tuersuntuoheti, T.; Mehmood, A.; Zhou, N.; Hao, S.; Wang, C.; Guo, Y.; Lin, W. A molecular docking and molecular dynamics simulation study on the interaction between cyanidin-3-O-glucoside and major proteins in cow's milk. *J. Food Biochem.* **2021**, *45*, No. e13570.

(21) Duran, T.; Minatovicz, B.; Bai, J.; Shin, D.; Chaudhuri, B. Molecular Dynamics Simulation to Uncover the Mechanisms of

Protein Instability During Freezing. *J. Pharm. Sci.* **2021**, *10*, 2457−2471.

(22) Billeter, S. R.; Eising, A. A.; Hünenberger, P. In *Biomolecular Simulation: The Gromos 96 Manual and User Guide*, 1996.

(23) Macpherson, J. A.; Theisen, A.; Masino, L.; Fets, L.; Anastasiou, D.; et al. Functional cross-talk between allosteric effects of activating and inhibiting ligands underlies PKM2 regulation. *eLife* **2019**, *8*, No. e45068.

(24) Sahihi, M. In-Silico Study on the Interaction of Saffron Ligands and Beta-Lactoglobulin by Molecular Dynamics and Molecular Docking Approach. *J. Macromol. Sci., Part B: Phys.* **2016**, *55*, 73−84.

(25) Mehranfar, F.; Bordbar, A. K.; Parastar, H. A combined spectroscopic, molecular docking and molecular dynamic simulation study on the interaction of quercetin with β-casein nanoparticles. *J. Photochem. Photobiol., B* **2013**, *127*, 100−107.

(26) Zhan, F.; Ding, S.; Xie, W.; Zhu, X.; Chen, Y.; et al. Towards understanding the interaction of β-lactoglobulin with capsaicin: Multi-spectroscopic, thermodynamic, molecular docking and molecular dynamics simulation approaches. *Food Hydrocolloids* **2020**, *105*, No. 105767.

(27) Sahihi, M.; Ghayeb, Y. An investigation of molecular dynamics simulation and molecular docking: Interaction of citrus flavonoids and bovine β-lactoglobulin in focus. *Comput. Biol. Med.* **2014**, *51*, 44−50.

(28) Liu, M.-Q.; Li, J.-Y.; Rehman, A. U.; Xu, X.; Gu, Z.-J.; Wu, R.-C. Laboratory Evolution of GH11 Endoxylanase Through DNA Shuffling: Effects of Distal Residue Substitution on Catalytic Activity and Active Site Architecture. *Front. Bioeng. Biotechnol.* **2019**, *7*, No. 350.